Journal of Engineering Technology
Volume 6, Issue 1, Jan. 2018, PP. 351-364

RESEARCH ARTICLE -ENGINEERNG TECHNOLOGY

A study on the registration strategy for a scant overlap problem with a robot

Zhi-Ren Tsai

Department of Computer Science & Information Engineering, Asia University, Taiwan.
Department of Medical Research, China Medical University Hospital, China Medical University, Taichung, Taiwan.

Abstract. This paper proposes a scant overlap registration strategy for 3D (three-dimensional) reconstruction of indoor map by using a robust, fast and efficient approach. First, a design methodology based on the use of an omnidirectional robot is proposed for the large-deformation data and scant overlap. Second, this robot uses vision-servo approach by a Kinect device for the purposes of avoiding obstacles and providing 3D data for walls. Third, experimental results illustrate that map's data sets with scant overlap cannot be registered directly by traditional registration methods. Finally, this study is based on the bee-colony algorithm to solve this registration problem.

Keyword: Registration; omnidirectional robot; Kinect; bee-colony algorithm; three-dimensional map; scant overlap.

1. Introduction. Artificial intelligence [1-3] has attracted much attention from both academic and industrial communities, and there have been many successful applications in different areas such as 6-DOF robot manipulator [3], image process [4], and big data analysis [5]. Artificial intelligence of reconstruction based on the registration of stereo-vision geometric data coming from large-overlap-modal images is essential for positioning and exploiting the complementary information provided by such images collected for image-guided procedures such as positioning in frameless neurosurgery. Potential applications of the proposed 3D alignment methodology include accurate positioning for medical surgery, omnidirectional robots, and invariant face recognition. The registration is usually defined as the procedure for aligning a model image with a reference image [1]. In previous robotic applications, the model or the template image is usually acquired initially from high-priced stereo-vision equipment and the reference image, or the collected data, which might be acquired from the same equipment during the motions of the robot. The model image is usually developed by merging with the next reference image, and so on. In this paper, the Kinematics-model-based control method [6, 7] is not able to deal with the self-guided problem in, for example, omnidirectional robots [8-10] on the desired trajectory on an uneven road. Without considering some unknown real situations and uncertain physical parameters such as the unknown payload, the torque of three motors, the consumption rate of the battery's electric energy, and situations of paved, unpaved or slippy roads with mud, the modeling research of controlling three-wheeled omnidirectional robots moving on a rocky road is difficult to implement. Moreover, many such specific control applications, as in this study, require inexpensive, stable and reliable strategies with the aid of a visual servo, stereo-vision process, 3D reconstruction and pattern recognition. Hence, an inexpensive stereo-vision module, Kinect [8], is used to help a robot avoid obstacles and provide its positioning by the registration. The Iterative Closest Point (ICP) algorithm [11, 12], together with the k-dimensional tree (K-D tree) search method [13], has been a popular registration scheme, and has been used in the alignment of human faces and general images [14]. However, these schemes are extremely sensitive to the choice of the initial guess for their relative rigid-body transform between the scant non-overlap data sets. Usually, a reliable solution requires multiple trials and manual removal of the non-overlap data sets and noise. Furthermore, the approaches in the literature demand huge computing power when the reference image or the model image contains a large data set, which is common in medical or robotic applications that extend the ICP algorithm with a so-called Grid Closest Point (GCP) technique [15] and Genetic Algorithm (GA) [16, 17] to improve runtime efficiency and the corresponding accuracy [18]. Nevertheless, this approach lacks robustness in registration results, is computationally intensive, and is stuck in the problem of scant overlap. In this paper, an optimization scheme with this omnidirectional

robot to solve this registration problem is proposed for its robustness. The consistent results are obtained for different initial poses in a proposed method that is fast enough to enhance the applicability of 3D registration in positioning applications of robots. The improvement is due to the introduction of an optimal spatial filter with the poses of a robot to select representative points to reduce the amount of data, and the application of an efficient artificial biological computation scheme for the search of global optimum coordinate transformation for scant overlap.

2. Registration Scheme. In order to simultaneously ensure robustness and rapidity, the proposed registration scheme is composed of an overlap identification stage, a registration stage and a recovering fine-tuning stage. In the overlap identification stage, the bee-colony algorithm is firstly used to find possible overlap of the data clusters, and then a truncation procedure is used to remove data points near the surface overlap in order to preserve only characteristic regions and to reduce faulty information. This is followed by a spatial sifter and a selection scheme with predicted overlap to further reduce the amount of data. In the registration stage, the bee-colony algorithm with GCP/ICP computation is implemented to find the alignment transformation. In the recovering fine-tuning stage, more complete overlap information is used for the ICP plus a K-D tree scheme to allow redundancy for precise registration, starting with the pose obtained in the second stage.

2.1. Pose Rectification. In order to cope with all of the possible orientations 3D images can pose, the images are firstly treated as data clusters on which the motions of robot are exploited to rectify their map poses. Specifically, the pose of a robot transforms the data into new coordinate systems such that the variance of the overlap data lies on the minimum situation. Fig. 1 demonstrates the result of a pose rectification of forward motion or right-turn motion applied on x-z image of points showing two principal axes of the data cluster from the center of the robot. The image was acquired with a Kinect stereo imaging sensor. Note that there is some superfluous noise data on its pavement and ceiling. This behavior is typical of measurements using a Kinect mounted on a robot; while providing high density data points, only right/left side regions are useful for the registration of maps. After both the model image and the reference image are posed according to their two principal axes, the data set is ready to be truncated to preserve only, say, 10 % of the original data set around the central part as a characteristic region for subsequent registration. The introduction of the motions of a robot and the truncation procedure can significantly reduce or completely avoid manual editing.

2.2. Bee-Colony Scheme. The improvement in efficiency of the proposed scheme depends largely on an effective sifter to preserve only representative data points that describe curvatures of overlap. All the other points, including faulty points and redundant data points, are to be removed. As shown in Figs. 1-2, the sifting procedure starts with the generating a vector, defined as follows: $c_{10} = [u_x, u_y, u_z, l_x, l_y, l_z, \theta, t_x, t_z, a_o]$, where a_o is the number of overlap points, and is larger than the specific threshold a_T. The cutting upper bounds u_x, u_y, u_z are along the x-axis, y-axis and z-axis, respectively; the cutting lower bounds l_x, l_y, l_z are along x-axis, y-axis and z-axis, respectively. θ is the angular prediction of the map pose by the turn-motion of robot; and a translation vector $\mathbf{t}(p) = [t_x, 0, t_z]^T$ is the position-offset prediction of the map pose by the shift-motion of the robot, where $p = [t_x, t_z]^T$. Since the Spatial filter acts as a 3-dimensional Filter, (S3F) is in the following presentation. The algorithm includes the following five steps:

Step 1: Set initial position p_0. Model image is now captured by the Kinect sensor at start point of robot.

Step 2: Next, the reference image is taken at end/big-turn point B of robot. Go to the registration algorithm in Section 2.3. Otherwise, go to the next step.

Step 3: Initialize the small angular offset Δ_θ, position offset p and the predicted truncating parameter vector c_{10} and go to Step 4.

Step 4: Detect whether the wall data exists in the front of map. If there is a front wall proximal to the robot, and the distance d between them is less than a specific threshold value d_T, then this robot changes

$\theta \leftarrow \theta + \Delta_\theta$ by right/left turn to a predicted angle $|\theta| < \theta_T$ (degree) automatically until $d > d_T$, where θ_T is a reasonable and specific threshold constant, and then go to Step 5. Otherwise, go to Step 2.

Step 5: Calculate new predicted position $p_0 \leftarrow p_0 + p$ of robot and go to Step 3.

2.3. Global Optimization Procedure. First, the partial parameters of the bee-colony algorithm have been listed in [8]. Specific variables of the scant overlap problem are described as: An objective function is defined as $O_B = \{c_{10}, [\theta_T, d_T, a_T] \in T\}$ which is related to Mean Square Error (MSE). The specific greedy nonlinear transform G improves the searching progress of the original bee-colony algorithm. $\mathbf{R}(\theta)$ is a rotation matrix with a predicted angle of map pose around the y-axis. $\mathbf{t}(p)$ is a translation vector with a position-offset prediction of map pose. Φ and Ψ are the model image and reference image, respectively. Φ' and Ψ' are the overlaps of model image and reference image, respectively. Φ'' and Ψ'' are the GCP overlaps of model image and reference image, respectively. And, there will be an objective function O_B with c_{10} to be optimized. The ith food source $x_i = [x_{i1}, x_{i2}, \ldots, x_{ij}, \ldots, x_{iD}]$ in x which could not be improved through limited trials t_R is abandoned by its employed bee, where x is the population of food sources. Each row of x matrix is a vector holding the parameters of this problem to be optimized. The number of rows of x matrix equals the constant N. New solution $v = [v_{11}, v_{21}, \ldots, v_{ij}, \ldots, v_{ND}]$ produced by x_{ij} and its neighbor x_{kj}, where k is the index of the adjacent solution of i's, and γ_{ij} is a random value in the range [-1,1]. The above equation generates a new greedy solution and uses GCP/ICP convergence error (MSE) with a reasonable amount of data after cutting its reasonable position with the rotation parameters range of translation matrix to assess their source location (in food) v_{ij}; and j is a randomly chosen parameter and k is a randomly chosen solution different from i. The optimum solution $y = \min_c [x_1, x_2, \ldots, x_c, \ldots, x_m]$ will be obtained due to its holding the optimal value x_c of each cycle in multiple cycles m. For the ease of presentation, the model image is denoted as Φ, and reference image is denoted as Ψ. The data sets collected after the procedure which is composed of truncation and filter are denoted as the overlaps Φ' and Ψ', respectively. Furthermore, the data sets collected after the Uniform Space Quantization (USQ) are denoted as Φ'' and Ψ'' by the GCP method, respectively. In this paper, the registration problem is simplified as the search of a rigid-body transformation that aligns these GCP overlaps of two images such that the average distance between corresponding data points is minimized by the GCP/ICP method as the result θ_{ICP} of θ. Specifically, the transformation is composed of a rotation matrix $\mathbf{R}(\theta)$ and a translation vector $\mathbf{t}(p) = [t_x, 0, t_z]^T$ that apply to each reference point $\mathbf{p}_i \in \Psi$: $\bar{\mathbf{p}}_i = \mathbf{R}(\theta)\mathbf{p}_i + \mathbf{t}(p)$, where $\bar{\mathbf{p}}_i \in \Gamma$, and $i = 1, 2, \ldots, O$, a transformed data set, and the rotation matrix $\mathbf{R}$ is constructed from rotation angles around the y-axis. Here, real numbers are used in the bee-colony algorithm directly to form food sources and to avoid a decoding operation. For the random optimization problem, a food source, denoted as x_i, is defined as a collection of the components of the unknown vectors and matrices to be found. That is, $x_i = c_{10}$. The correspondence between the two data sets is actually unknown before successful registration; otherwise, the task can be done in one step. Hence, performance evaluation is based on the average distance of closest points between the two data sets. If the number of data points in the model image, M, is smaller than that of the reference image, then the MSE value (mm) can be defined as:

Journal of Engineering Technology
Volume 6, Issue 1, Jan. 2018, PP. 351-364
RESEARCH ARTICLE -ENGINEERNG TECHNOLOGY

$$\text{MSE} = \begin{cases} \frac{1}{M}\sum_{k=1}^{M}[\min_{\bar{\mathbf{p}}\in\Gamma}\|\mathbf{q}_k - \bar{\mathbf{p}}\|], & \text{if } a_0 \ge a_T \text{ and } |\theta - \theta_{ICP}| \le 0.05\theta_T, \\ 10d_1, & \text{if } a_0 < a_T,\ |\theta - \theta_{ICP}| > 0.05\theta_T \text{ and } |M - O| > 0.2a_T, \\ d_1, & \text{if } a_0 < a_T,\ |\theta - \theta_{ICP}| \le 0.05\theta_T \text{ and } |M - O| \le 0.2a_T, \\ 0.1d_1, & \text{if } a_0 \ge a_T \text{ and } |\theta - \theta_{ICP}| > 0.05\theta_T, \end{cases}$$

where d_1 =3600(mm) is the maximum effective distance of Kinect depth. The details of twelve steps of this algorithm are noted in [8], and a food source is chosen with a probability which is proportional to its quality. Probability values $P_i(\bar{f}_i)$ are calculated by using fitness values $\bar{f}_i$ and normalized by dividing maximum fitness value $\max_i \bar{f}_i$. So, calculate the probability values $P_i(\bar{f}_i)$ by x_i as follows:

$$P_i = \frac{0.9\bar{f}_i}{\max_i \bar{f}_i} + 0.1 \in P_B, \text{ where } \bar{f}_i(G) = \frac{d_1}{f_i(G)},$$

where d_1 =3600(mm) is the maximum effective distance of Kinect depth.

2.4. Recovering Fine-Tuning Stage. In the third stage, the intermediate solution obtained in the second stage is used as the initial pose for an ICP plus K-D tree scheme. This three-stage approach is due to an intrinsic problem of ICP in that the algorithm iterates to the local minimum closest to the starting pose and with scant overlap. During this stage, data sets obtained just after the sifting, Φ' and Ψ', are used for accurate registration, instead of Φ'' and Ψ''. Also, the computationally intensive K-D tree procedure is only executed once in this stage. Finally, this stage recovers all the original data sets and merges them into a complete map as a reconstruction procedure.

2.5. Reconstruction Procedure. To clarify the overall three-stage procedure, the complete registration procedure is summarized by the following steps:

Step 1: Apply the pose prediction and rectification, using the motions of the robot and a selected characteristic region of the model image Φ and the reference image Ψ.

Step 2: Truncate Φ and Ψ to preserve only their overlap parts by the bee-colony algorithm.

Step 3: Apply the overlap to the data sets. The results are denoted as Φ' and Ψ' by the bee-colony algorithm, respectively.

Step 4: Apply the Uniform Space Quantization (USQ) to the data sets by GCP. The results are denoted as Φ'' and Ψ'', respectively.

Step 5: Calculate the K-D tree data structure of Φ''.

Step 6: Use the bee-colony algorithm to find the optimum place in food, defined as c_{10}, such that the fitness is maximized for data sets Φ'' and Ψ''.

Step 7: Calculate the K-D tree data structure of Φ'.

Step 8: Apply the ICP plus K-D tree scheme to data sets Φ' and Ψ' for fine-tuned registration, starting with the initial pose obtained in Step 6.

Step 9: Use the pose of the fine-tuned registration to recover all of the original data sets and merge them into a complete/reconstructed map Ω.

2.6. Positioning Scheme of Robot. According to the following switching strategy, the obstacle avoidance and positioning control of a robot can greatly reduce the complexity of the design.

Step 1: Measure 3D data Ψ by Kinect.

Step 2: Sift and delete the noise by some conditions as $u_x, u_y, u_z, l_x, l_y, l_z$.

Step 3: Project the 3D data points on to a 2D plane of x-y axes, and transform them into 2D data.

Step 4: Set a threshold value A_T. Calculate the area A of 2D data. If $A \le A_T$, then start forward walking

motion. Otherwise, make robot right-turn walk to avoid the obstacles.

Step 5: Compute the registration of the 3D data Ψ and a reconstructed map Ω by the pose prediction and rectification, and appropriate truncation of Ω.

Step 6: Use the **R**,**t** of this registration to calculate the position of the robot, as shown in Fig. 2c.

3. Comparison Studies. For the maps: the model image and reference image have about 187852 points of surface data extracted from a Kinect. They have a complete overlap to be registered directly by ICP. But, the registration method of scant overlap is still faster than ICP. The bee-colony algorithm has been implemented for this example with the design parameters: the population size of bees is 50. Elitism is also implemented with one best food source preserved for the next cycle. Also, the bee-colony algorithm is executed for only 25 cycles to save time, and its searching result,

$$y = [u_x, u_y, u_z, l_x, l_y, l_z, \theta, t_x, t_z, a_o]$$
$$= [3149.6, 398.2, 7951.8, 655.5, 56.4, 9.6, 87.8, 4.9, 6318.8, 3823] \in c_{10},$$

is demonstrated in Fig. 2. Finally, this reconstructed map that uses the **R**,**t** of this continuous registration for the continuous motions of a mobile robot is shown in Fig. 2c. To illustrate the validity of the proposed S3F and greedy nonlinear transform, the first comparison of the method with the Grid Closest Point (GCP) technique GCP/GA is demonstrated in Fig. 3. Note that in the GCP/GA case, to comply with the maximization formulation and linear transform of real numbers in the GCP/GA evolutionary computation, the fitness value $\bar{f}_i(x_i)$ defined by the linear transform $f_i(x_i) \neq f_i(G)$, where $f_i(G)$ is the greedy nonlinear transform, is inversely proportional to the average distance between the points in the model set, $\mathbf{q}_k \in \Phi$, and their corresponding closest points, $\bar{\mathbf{p}}$, in the transformed reference data set. To accelerate the search of the nearest $\bar{\mathbf{p}}$ for each $\mathbf{q}_k$, the reference image points are sorted in the K-D tree structure before transformation and evaluation of the fitness function. The optimization problem is then defined as finding c_{10} that maximizes the fitness value $\bar{f}_i(x_i)$. The second comparison of the method with the Iterative Closest Point (ICP) plus K-D tree scheme is demonstrated in Fig. 4. In the following studies, the proposed registration scheme is to be compared with the ICP and the GCP/GA scheme which is composed of a so-called Grid Closest Point (GCP) transform and Genetic Algorithm (GA). These methods will be briefly denoted as "Bee-Colony Scheme", "GCP/GA" and "ICP" in the following discussion, in Table 1. The registration time of Table 1 shows the effect of data reduction after truncation and selection using the proposed sifter. Comparing the capture times by Kinect, registration times, the time of registration, and registration result of the three cases, it is clear that the bee-colony algorithm is more robust and efficient in finding the best aligning poses than the other two algorithms. The efficiency is not only demonstrated in convergence speed but also in the achieved cost value for this practical problem by low-price Kinect. In order for the robot to obtain the wall data sets without touching the wall, this paper considers the servo control problem of guiding and positioning a robot by an obstacle avoidance scheme. Further, effectiveness of the approach is demonstrated by a comparison of correctness with two popular algorithms, the GCP/GA (Grid Closest Point (GCP) technique and Genetic Algorithm (GA)) and Iterative Closest Point (ICP) methods. Finally, the quality of registration for a benchmark data of [19] is shown in Fig. 5.

4. Conclusions. In this paper, a fast and accurate 3D registration scheme is proposed for the scant overlap of data sets. To find an equilibrium between speed and robustness, the non-overlap of data sets should be adequately reduced and global optima ensured. This goal is achieved by dividing the registration process into three stages. Effectiveness of the proposed approach is demonstrated by a practical map registration problem compared with the GCP/GA scheme and ICP. The bee-colony scheme succeeds in each run with equal results. On the contrary, the results of comparison schemes vary dramatically. In comparison, total execution time is reduced from 243 units to 14 units. Results of the example problems show that this approach outperforms the typical scheme found in the literature with greatly reduced execution time and a steady high registration

accuracy.

Acknowledgements. The author would like to thank the Ministry of Science and Technology, R.O.C. for the support under contracts: MOST 106-2632-B-468-001 and 106-2221-E-468-023. My gratitude also goes to Dr. Chun-San Wang, Asia University.

References

[1] A. Gunasekaran, E.W.T. Ngai, Expert systems and artificial intelligence in the 21st century logistics and supply chain management, Expert Systems with Applications 41 (2014) 1–4.
[2] P. Babu, V. Rajamani, K. Balasubramanian, Multipeak mean based optimized histogram modification framework using swarm intelligence for image contrast enhancement, Mathematical Problems in Engineering 2015 (2015) 1-14.
[3] R.M. Asl, Y.S. Hagh, R. Palm, Robust control by adaptive non-singular terminal sliding mode, Engineering Applications of Artificial Intelligence 59 (2017) 205–217.
[4] Z. Zhang, F. Li, M. Zhao, L. Zhang, S. Yan, Robust neighborhood preserving projection by nuclear/L2,1-norm regularization for image feature extraction, IEEE Transactions on Image Processing 26 (2017) 1607-1622.
[5] A. Moreno, T. Redondo, Text analytics: the convergence of big data and artifcial intelligence, International Journal of Interactive Multimedia and Artificial Intelligence 3 (2016) 57-64.
[6] T.K. Tanev, Geometric algebra based kinematics model and singularity of a hybrid surgical robot, Advances in Robot Kinematics 4 (2016) 431-440.
[7] H. Jin, Q. Chen, Z. Chen, Y. Hu, J. Zhang, Multi-LeapMotion sensor based demonstration for robotic refine tabletop object manipulation task, CAAI Transactions on Intelligence Technology 1 (2016) 104-113.
[8] Z.R. Tsai, Robust Kinect-based guidance and positioning of a multidirectional robot by Log-ab recognition, Expert Systems with Applications 41 (2014) 1271–1282.
[9] G. Ishigami, K. Iagnemma, J. Overholt, G. Hudas, Design, development, and mobility evaluation of an omnidirectional mobile robot for rough terrain, Journal of Field Robotics 32 (2015) 880–896.
[10] O.Y. Ismael, J. Hedley, Analysis, design, and implementation of an omnidirectional mobile robot platform, American Scientific Research Journal for Engineering, Technology, and Sciences 22 (2016) 195-209.
[11] Y. Fan, H. Cheng, B.B. Xing, Z. Chao, L.W. Jing, Study on a stitching algorithm of the iterative closest point based on dynamic hierarchy, Journal of Optical Technology 82 (2015) 28-32.
[12] P. Krusi, B.Bucheler, F. Pomerleau, U. Schwesinger, R. Siegwart, P. Furgale, Lighting-invariant adaptive route following using iterative closest point matching, Journal of Field Robotics 32 (2015) 534–564.
[13] X.S. Liu, S. Zhou, H. Li, K. Li, Bidirectional scale-invariant feature transform feature matching algorithms based on priority k-d tree search, International Journal of Advanced Robotic Systems 2017 (2017) 1-12.
[14] R.Y. Takimoto, M. de Sales Guerra Tsuzuki, R. Vogelaar, T. de Castro Martins, A.K. Sato, Y. Iwao, T. Gotoh, S. Kagei, 3D reconstruction and multiple point cloud registration using a low precision RGB-D sensor, Mechatronics 35 (2016) 11–22.
[15] S. Auer, C.B. Macdonald, M. Treib, J. Schneider, R. Westermann, Real-Time fluid effects on surfaces using the closest point method, Computer Graphics Forum 31 (2012) 1909–1923.
[16] M. Qiu, Z. Ming, J. Li, K. Gai, Z. Zong, Phase-change memory optimization for green cloud with genetic algorithm, IEEE Transactions on Computers 64 (2015) 3528-3540.
[17] N. Fang, J. Zhou, R. Zhang, Y. Liu, Y. Zhang, A hybrid of real coded genetic algorithm and artificial fish swarm algorithm for short-term optimal hydrothermal scheduling, International Journal of Electrical Power & Energy Systems 62 (2014) 617-629.
[18] S.M. Yamany, M.N. Ahmed, A.A. Farag, A new genetic-based technique for matching 3-D curves and surfaces, Pattern Recognition 32 (1999) 1817-1820.
[19] MathWorks, 3-D Point Cloud Processing, https://www.mathworks.com/help/vision/3-d-point-cloud-processing.html, 2017.

Journal of Engineering Technology
Volume 6, Issue 1, Jan. 2018, PP. 351-364
RESEARCH ARTICLE -ENGINEERNG TECHNOLOGY

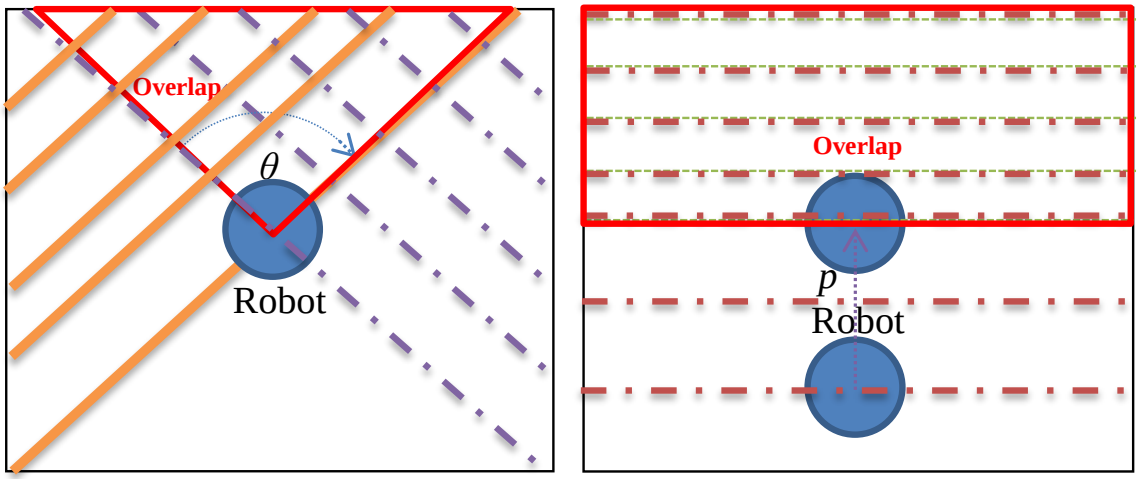

(a) (b)

Figure 1. Red region is the predicted overlap of right-turn moving mode (a) and shifting mode (b) of the robot [8].

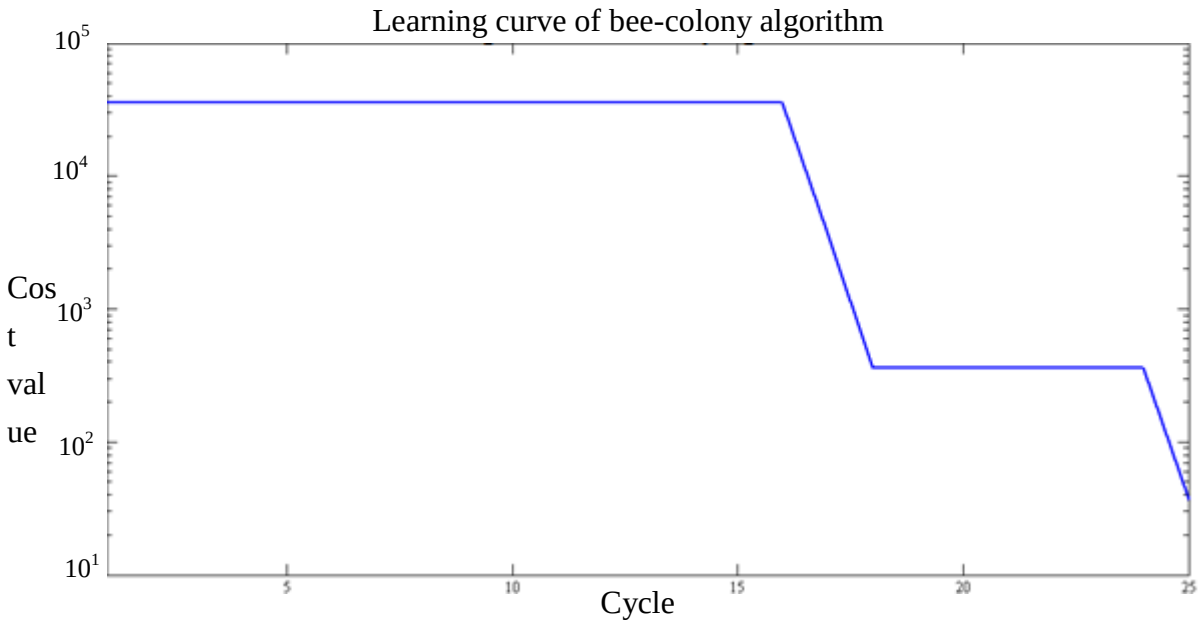

(a)

Journal of Engineering Technology
Volume 6, Issue 1, Jan. 2018, PP. 351-364
RESEARCH ARTICLE -ENGINEERNG TECHNOLOGY

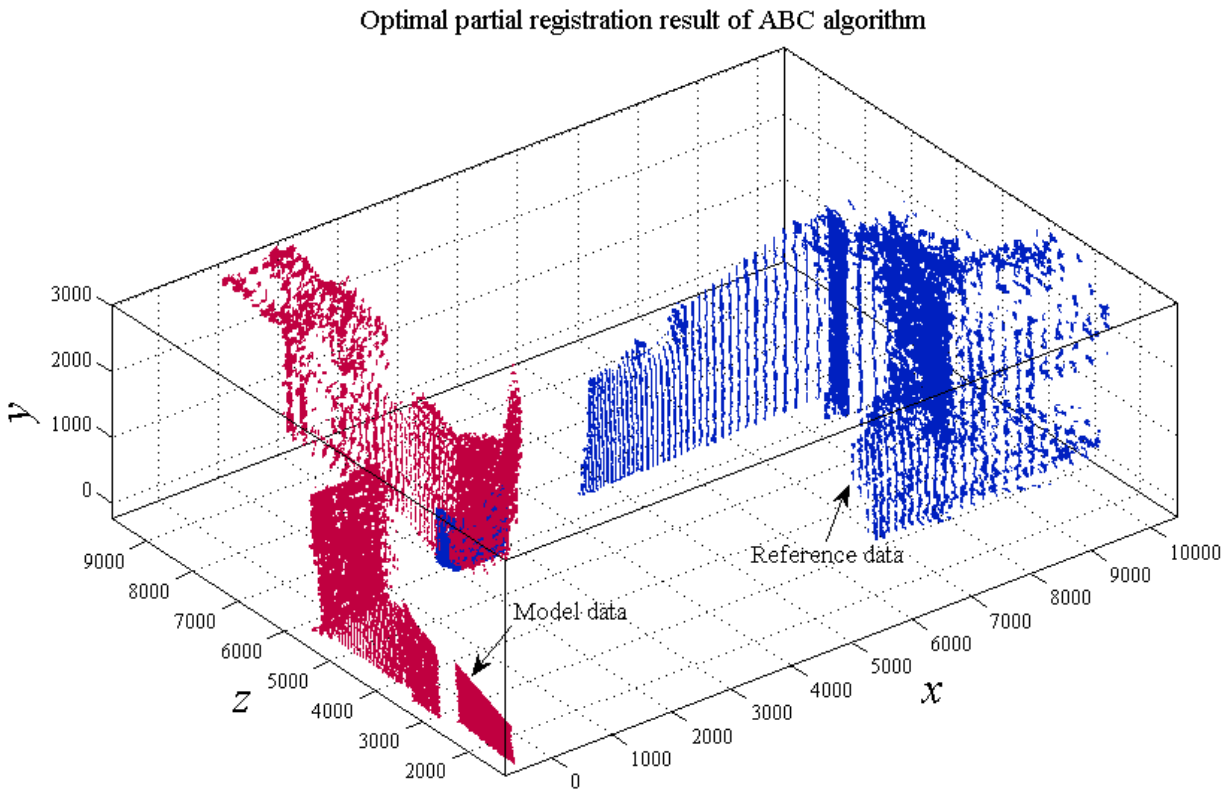

(b)

Figure 2. Cost value of learning curve (a) is defined as MSE; optimal registration result (b) of scant overlap data is obtained by using the bee-colony algorithm.

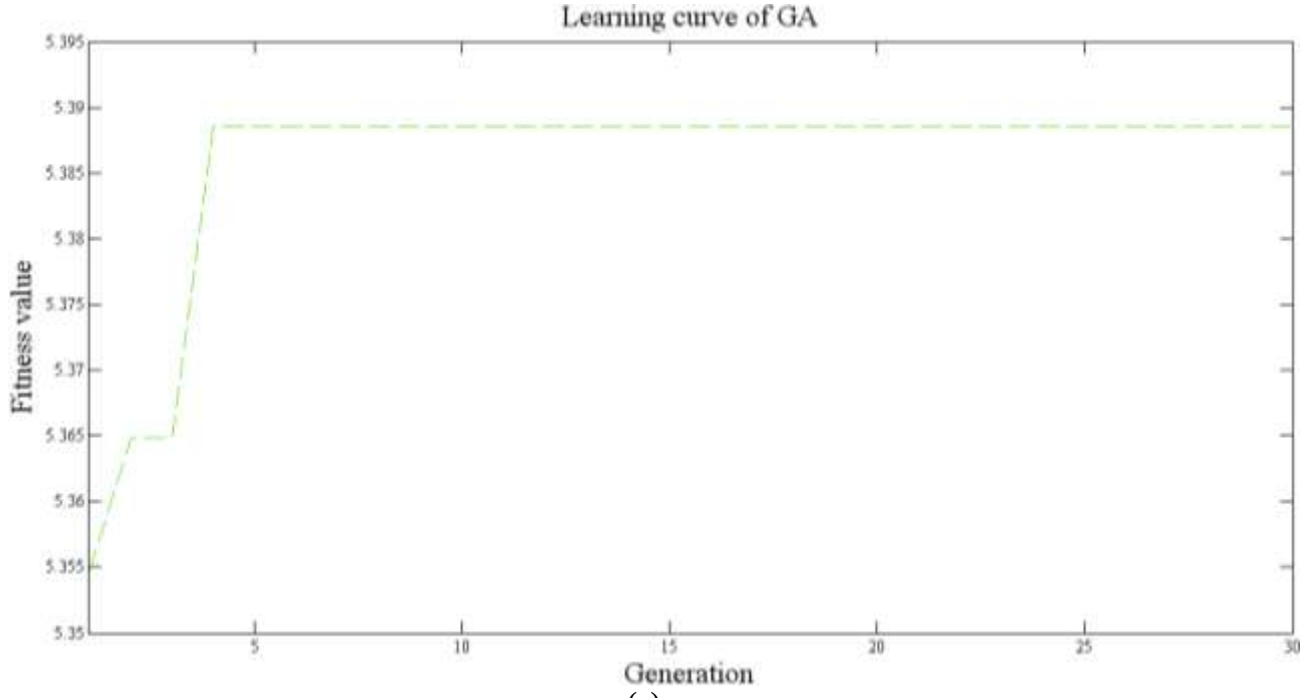

(a)

Journal of Engineering Technology
Volume 6, Issue 1, Jan. 2018, PP. 351-364

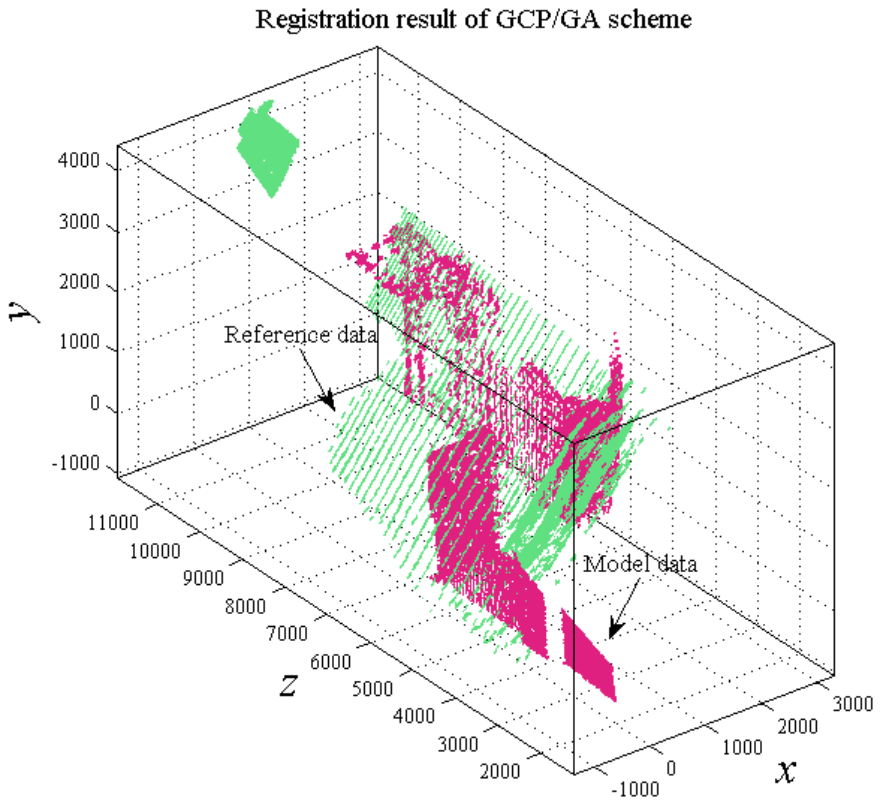

(b)

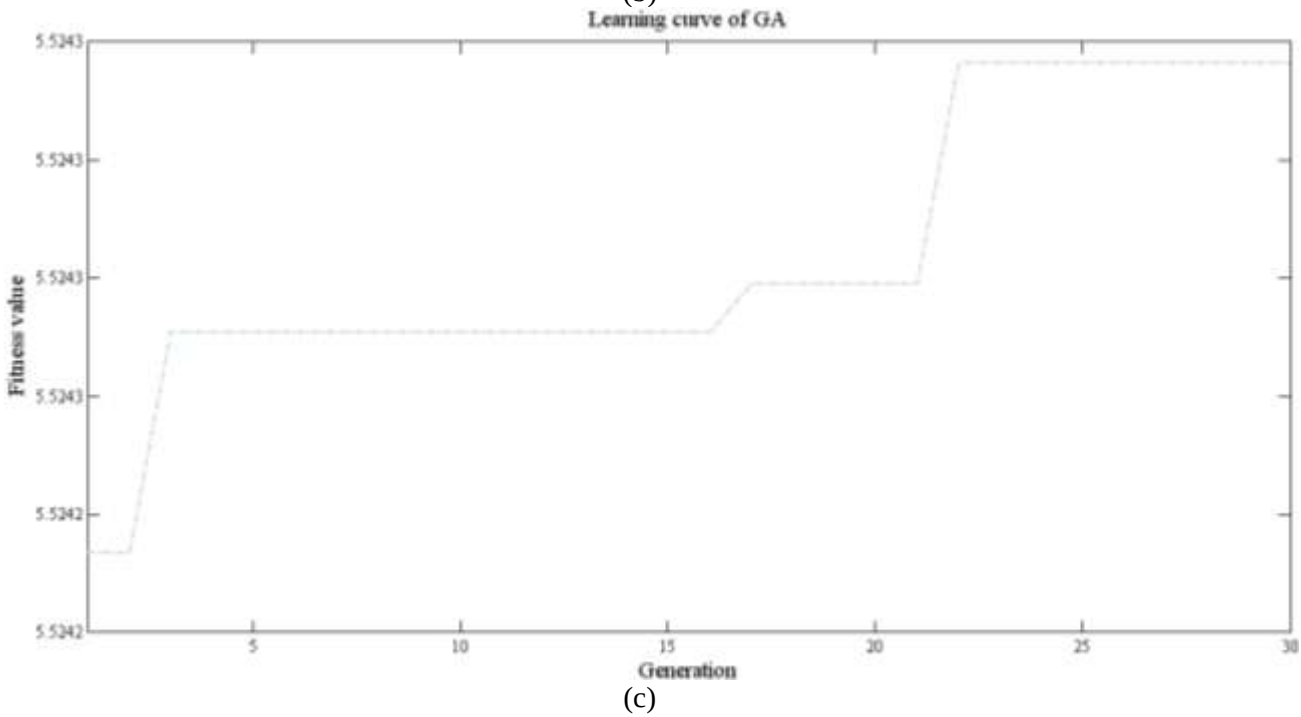

(c)

Journal of Engineering Technology
Volume 6, Issue 1, Jan. 2018, PP. 351-364
RESEARCH ARTICLE -ENGINEERNG TECHNOLOGY

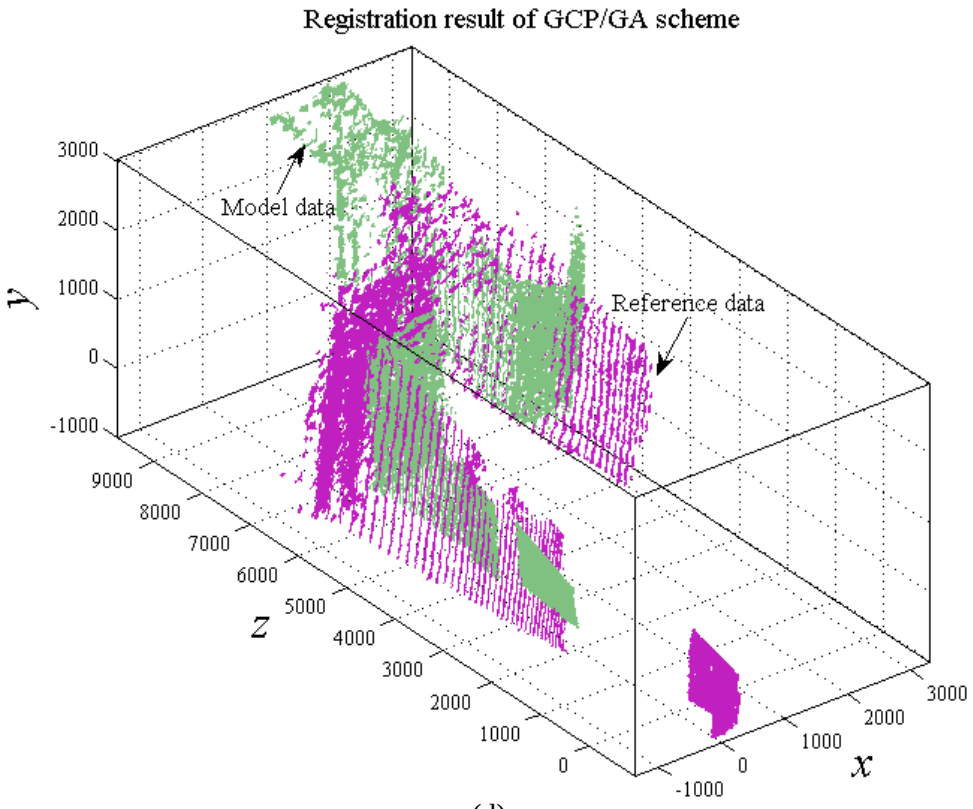

(d)

Figure 3. Fitness value of learning curve (a) is $\bar{f}_i(x_i)$ at the first run of GCP/GA; registration result (b) of GCP/GA scheme is obtained at the first run; learning curve (c) is recorded at the second run of GCP/GA; registration result (d) of GCP/GA scheme is obtained at the second run.

Journal of Engineering Technology
Volume 6, Issue 1, Jan. 2018, PP. 351-364

RESEARCH ARTICLE -ENGINEERNG TECHNOLOGY

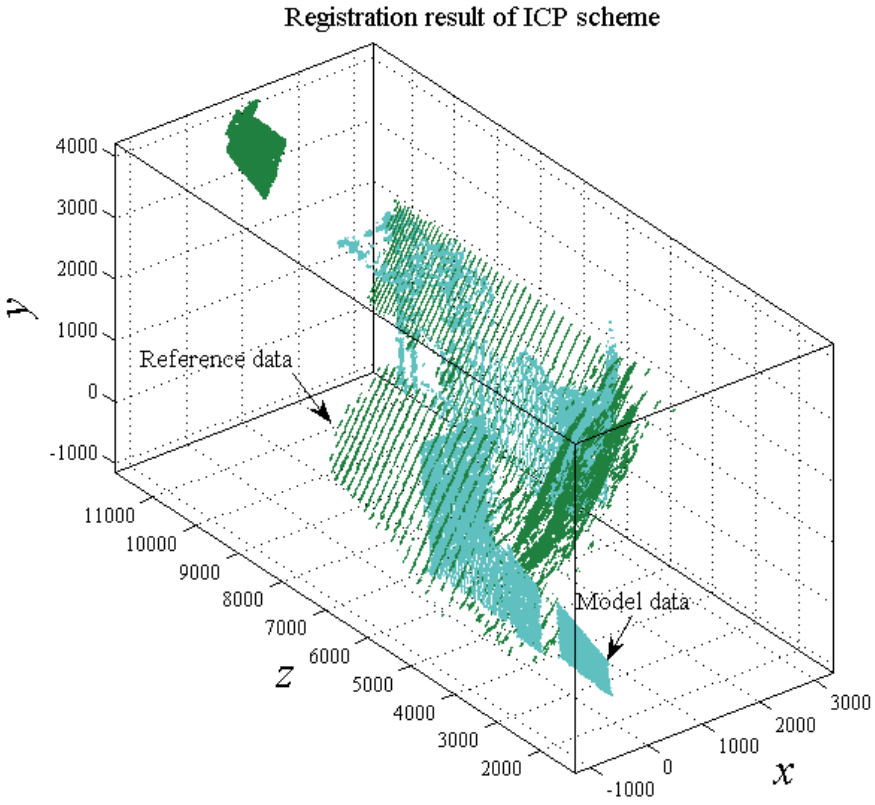

Figure 4. Registration result of ICP scheme.

Performance \ Cases	GCP/GA	ICP	Bee-Colony Scheme
Capture times by Kinect	38	38	2
Registration times	37	37	1
Registration time (1 unit = 9.8289 sec)	About 243 units	About 35 units	About 14 units
Registration result	Failure	Failure	Success

Table 1. Performance comparisons of three cases.

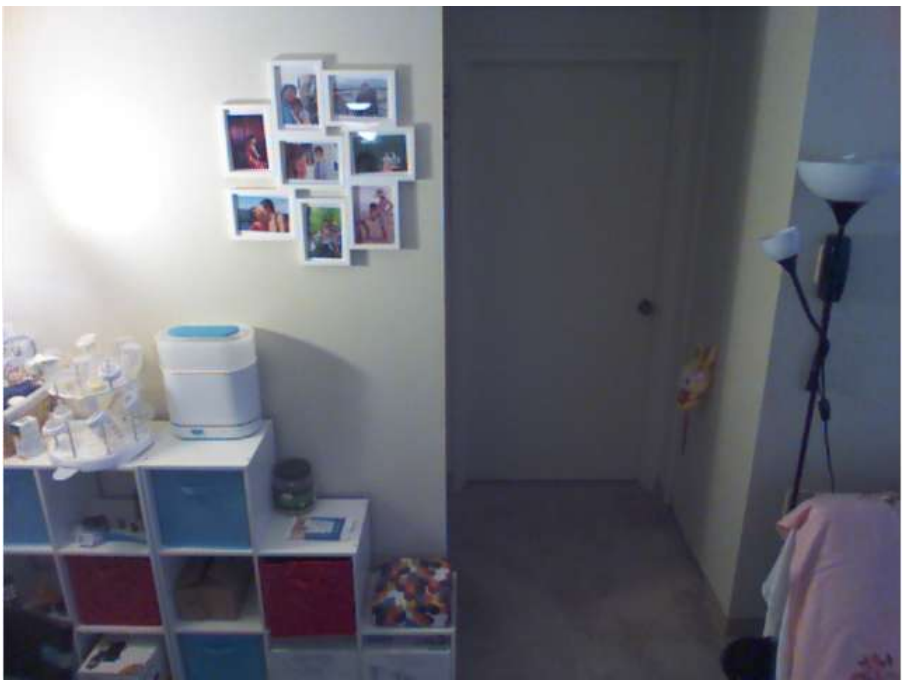

Journal of Engineering Technology
Volume 6, Issue 1, Jan. 2018, PP. 351-364

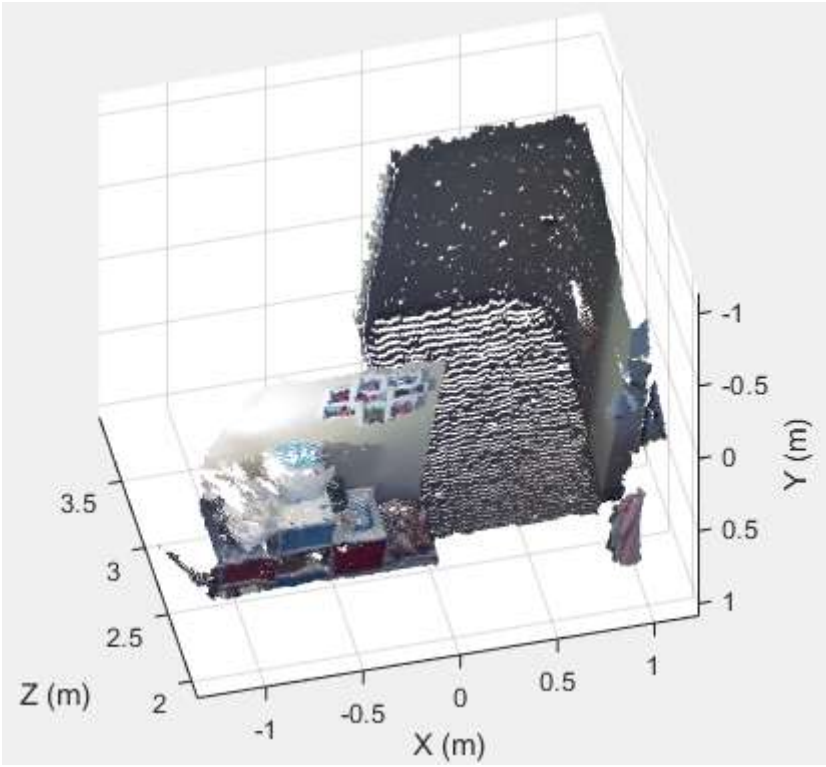

(a)

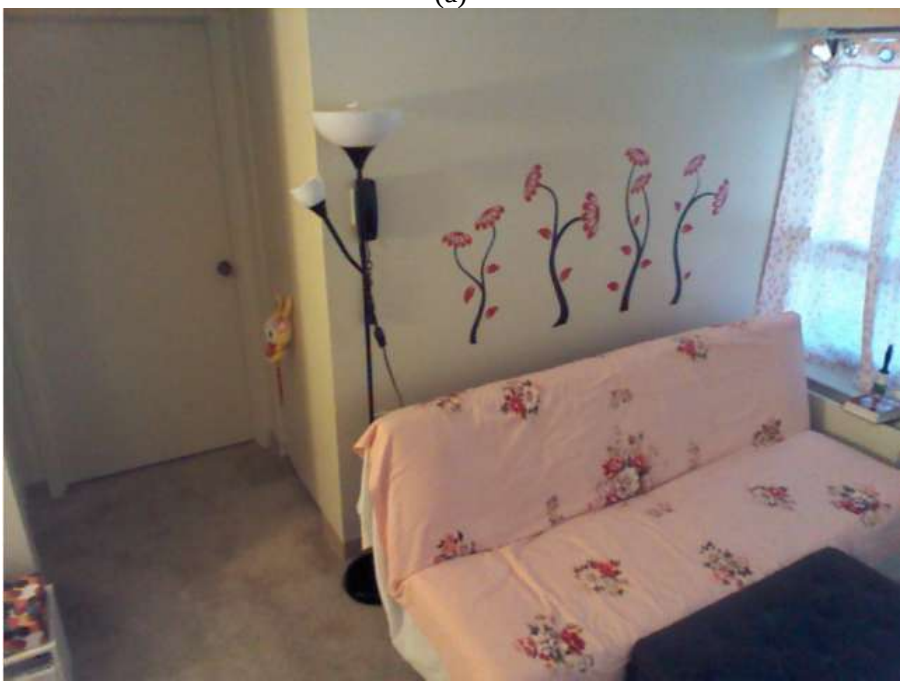

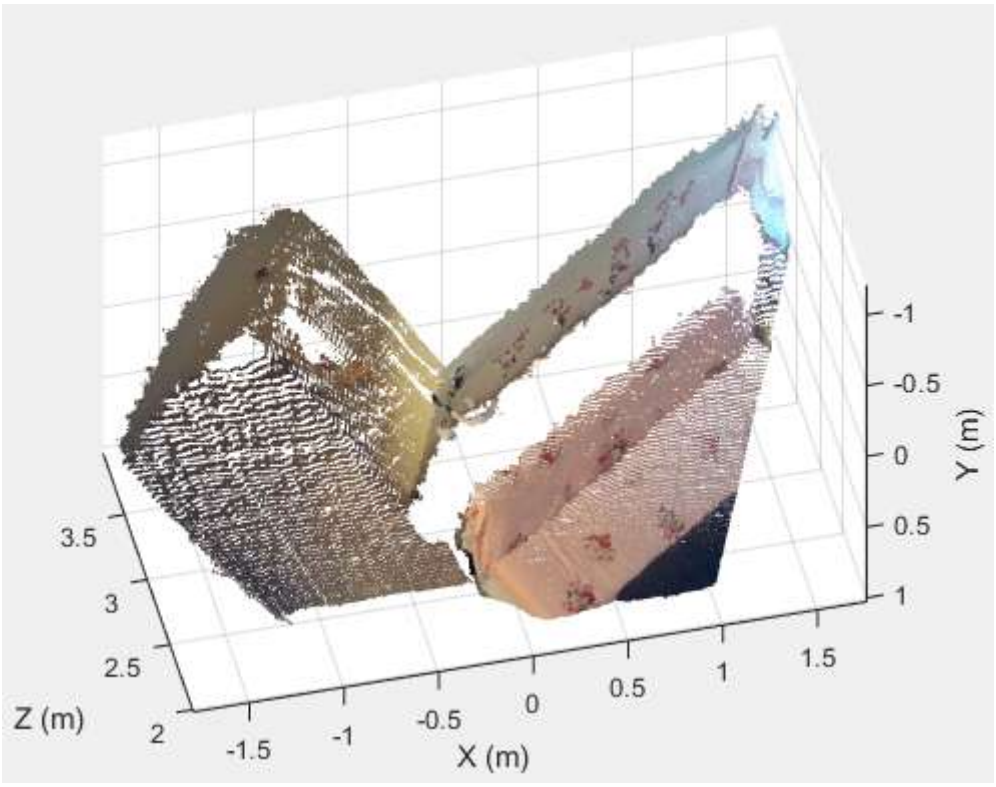
3.5
3
2.5
2
Z (m)
-1.5
-1
-0.5
0
0.5
1
1.5
X (m)
-1
-0.5
0
0.5
1
Y (m)

(b)

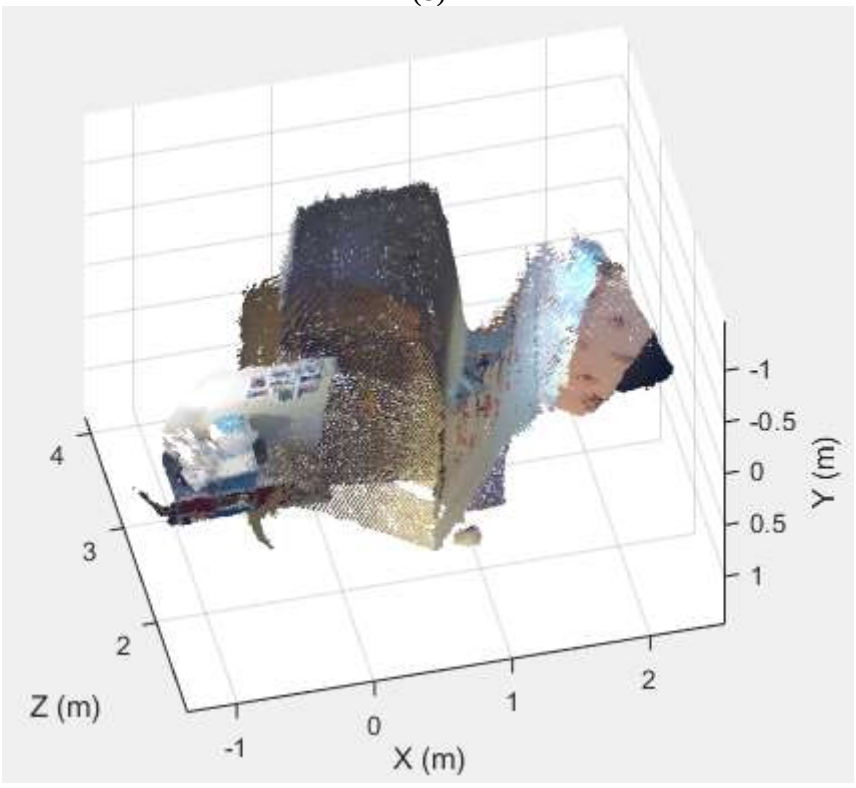
4
3
2
Z (m)
-1
0
1
2
X (m)
-1
-0.5
0
0.5
1
Y (m)

(c)

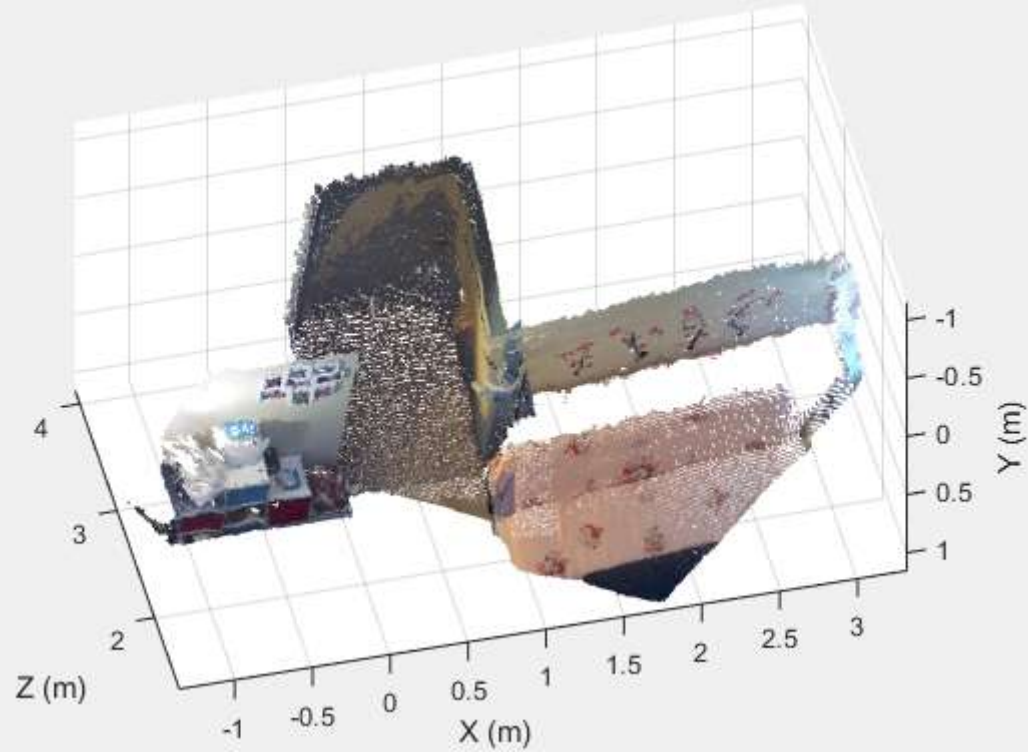

(d)

Figure 5. (a) The reference frame (frame 1) captured with a Kinect device is the reference coordinate system defined by the first image and point cloud. (b) The frame 2 captured with a Kinect device is the moving frame measured by the next image and point cloud. (c) The visualized ICP registration result is shown by frame 1 and frame 2. (d) The registration performance of the proposed method is obtained by frame 1 and frame 2.